

# Diagram technique for phonon turbulence

S. V. Gantsevich, V. D. Kagan, and P. Katilyus

*A. F. Ioffe Physico-technical Institute, USSR Academy of Sciences*

(Submitted March 11, 1974; revised June 11, 1974)

Zh. Eksp. Teor. Fiz. 67, 1765-1784 (November 1974)

A diagram technique is developed for describing the interaction between longwave phonons under sound instability conditions. A kinetic equation for phonons is derived in which, owing to strong dissipation of energy by electrons, the major role is played by the four-phonon interaction via the electron subsystem. Variation in the nature of the interaction on narrowing of the beam below the limit of applicability of the kinetic equation is analyzed. As the beam narrows, the role of three-phonon processes increases; in a coherent beam these processes enter the interaction via the second harmonic. The processes responsible for alteration of the statistical properties on transition from noise to signal are specified.

## 1. INTRODUCTION

In the present work a diagram technique is derived from first principles (quantum statistics), which allows us to describe the averaged behavior of classical vibrational degrees of freedom of a system for the case when these are sufficiently far from equilibrium. The technique is used to study sound (phonon) turbulence in solids. In our approach, initial quantum-statistical averaging suffices to describe the stochastic motion of waves in terms of their intensity (the diagram technique contains only intensities), whereas in the usual description of turbulent motion the averaging is performed over the phases of already enhanced oscillations<sup>[1-4]</sup>. The advantage of initial-averaging lies not so much in its greater consistency as in the fact that the law of the decoupling of the higher correlators is known exactly beforehand, i.e., one knows exactly the statistical properties of the waves involved. The statistical properties of developed oscillations are not a priori known and the decoupling is fraught with a certain hazard: it may be erroneous if the statistical properties vary in the course of the nonlinear interaction. Such a variation of the statistical properties may occur, if, in the process of amplification, a large intensity is concentrated in one or several very narrow regions of the spectrum—the “self-action” of waves becomes comparable to their “interaction.” As we shall see, our diagram technique provides a convenient method for analyzing the nonlinear processes which occur on narrowing the intensive noise beams—the processes which under certain conditions may lead, say, to separation of a signal from the enhanced thermal noise. (We shall especially discuss this latter point in another work.)

We shall carry out the analysis using as a concrete example an electron-phonon system. It is known in such a system there can occur a phonon instability brought about by, say, the drift of conduction electrons: if a semiconductor is located in a sufficiently strong external electric field, so that the electron drift velocity exceeds the speed of sound, then the electron-phonon interaction can lead to phonon amplification instead of damping (i.e., cause instability) and enhance the thermal noise. Since the amplification factor is usually maximal at a comparatively low frequency (in a piezoelectric semiconductor noises with wavelengths of the order of reciprocal Debye radius have the maximal growth rate), it is precisely the classical region of the phonon spectrum which is enhanced. This raises the question of describing the interaction between enhanced classical noises, i.e., of developing a theory of phonon turbulence. For this purpose, we use the usual quantum diagram describing the kinetics of an electron-phonon system (the Konstantinov-Perel' technique, to be specific) to

derive a technique adapted specially for the description of low-frequency and long-wavelength phonons ( $\hbar\omega_{\mathbf{q}} \ll \epsilon_{\mathbf{p}}$ ,  $\hbar\mathbf{q} \ll \mathbf{p}$ , where  $\mathbf{q}$  and  $\omega_{\mathbf{q}}$  are the phonon wave vector and frequency;  $\mathbf{p}$  and  $\epsilon_{\mathbf{p}}$  are the average electron quasi-momentum and energy). We shall show that the technique describing the nonlinear interaction between enhanced sound noises is particularly simple when the latter are sufficiently far from equilibrium, namely when the products of the quasi-classical parameter by the phonon number are large (i.e.  $N_{\mathbf{q}}\hbar\omega_{\mathbf{q}}/\epsilon_{\mathbf{p}} \gg 1$  and  $N_{\mathbf{q}}\hbar\mathbf{q}/\mathbf{p} \gg 1$ ). Under these conditions our technique will prove equivalent in a certain sense to that of Wyld<sup>[1]</sup>. The latter was derived by averaging over phases of classical equations of motion and employed to describe the classical theory of turbulence in liquids.

Let us now outline the results of direct application of our diagram technique, which are expounded in the present paper.

1. An equation for weak phonon turbulence is derived from first principles, and limits of its applicability are stipulated (such an equation in the hydrodynamic limit has been obtained earlier, using phase averaging, by V. Gurevich, Laikhtman, and one of us<sup>[4]</sup>). Here we would like to emphasize the following point. Linear theories of growing noise involve, along with the amplification factor, a “source” which determines the initial noise level (pre-exponential factor in the solution). In order to take the nonlinearity into account one usually looks for corrections to the amplification and in one way or another avoids the question of nonlinear corrections to the source, since these are extremely difficult to incorporate in the averaging over phases. In the present work we are concerned only with the strongly non-equilibrium noise when the source itself is immaterial, let alone corrections to it. We would like to point out, however, that in the framework of our method these corrections can be systematically taken into account, and we believe that this is important in principle.

2. Recently, Wonneberger<sup>[5]</sup> made an attempt to build a theory of enhanced turbulence in a phonon system. Our investigation reveals that only a fraction of significant diagrams had been summed over, and we shall point to a class of left-out diagrams having the same order of magnitude as those taken into account. The absence of an easily summable sequence of diagrams reduces our hope to build a theory of enhanced turbulence; however, certain relations can still be obtained even under strongly nonlinear conditions. Such is, for example, the Weinreich relation between the (now nonlinear) amplification factor and the acousto-electric current.

3. Some time ago<sup>[4]</sup> the problem of building a theory of interaction between a sound signal and a sound noise

was pointed out as an important one. We show that the problem of calculating the effect of the noise on the amplification of a weak signal can be reduced to the above, namely to calculation of the nonlinear coefficient of noise amplification (since the latter is connected with the response of a system in which noises are growing to a weak external acoustic or electric perturbation).

4. We shall analyze the distinction between the interaction in a relatively narrow noise beam and the nonlinear self-action of a coherent sound wave, which remained unexplained for a number of years. The question consists in the following. On the one hand, the nonlinear amplification was calculated in<sup>[6]</sup> for a sound signal (i.e., for an excitation of a given intensity concentrated in such a narrow region of the phonon spectrum that at the typical amplification times it behaves like one mode). On the other hand, the coefficients of interaction between noise modes were calculated in<sup>[4]</sup>. It has been pointed out already in<sup>[4]</sup> that the analytic expression for the coefficient of interaction of two noise modes does not go over into the self-action coefficient of the signal mode evaluated in<sup>[6]</sup> when the separation between the modes formally approaches zero. It is evident that the discrepancy is due to the fact that the noise approach (averaging over phases) is not applicable to a very narrow beam of which a signal is the limiting case. It seems, however, that nobody has understood what really happens when the beam is narrowed down beyond the limits of applicability of the noise approach. The diagram analysis enabled us to answer this question with little effort. We shall show that in a narrow beam there comes into play a new type of interaction which is insignificant in a sufficiently wide beam. In a wide beam, as has been ascertained in<sup>[4]</sup>, the dominant role is played by the four-phonon interaction phonon scattering by each other ("two into two") through the mediation of the electron system. In terms of the coupling constant the scattering proves to be more effective than the more usual "Peierls" processes of one-into-two decay with the subsequent two-into-one coalescence, i.e., than the three-phonon interaction. We have found, however, that this holds only for a wide beam. Closely spaced modes interact effectively in both "non-Peierls" and Peierls manner, since the latter interaction has a resonance character for close modes. In a beam that is narrow beyond the limits of applicability of the noise equation, the resonant Peierls contribution increases and becomes comparable in order of magnitude with the non-Peierls one. Adding the Peierls terms to the corresponding non-Peierls ones and then letting the beam width go to zero, we obtain, to within a factor of 2, the result of the "signal" theory<sup>[6,11]</sup>.

5. The less striking, but nevertheless of a profound nature, discrepancy between the numerical coefficients in the analytic expressions for the amplification of the nonlinear signal and that of the noise (the above-mentioned factor of 2) can also be attributed to the different number of diagrams in the "noise" and "signal" theories (more precisely, the number of ways to close the "signal" diagrams). This difference reflects the dissimilarity between statistical properties of signal and noise, and we have succeeded in identifying the processes responsible for reorganization of these statistical properties on going from signal to noise. We do not claim here that we have solved the cardinal problem, which is the quantitative description of the noise-to-signal transition (which, incidentally, cannot in principle

be described by a closed equation for the mean intensities—precisely because of the change in the statistical properties during the transition). Nevertheless, we believe that our analysis sheds some light on the physics of the interaction in a very narrow beam.

## 2. THE DIAGRAM TECHNIQUE

Consider a semiconductor in a strong electric field which causes drift of the electrons (and may "heat" them). The electrons interact with a thermostat, whose role is played by impurities and shortwave nonamplifiable phonons ( $\hbar q \sim p$ ). We assume that the usual validity criterion of a kinetic equation

$$\hbar/\varepsilon_p \tau_n \ll 1 \quad (2.1)$$

is satisfied for the electrons ( $\tau_p$  is the characteristic electron relaxation time). The electron system is assumed nondegenerate.

Our task is to calculate the intensity of longwave phonons interacting with such an electron system. The intensity will be described by the number of phonons  $N_q(t)$  with the wave vector  $q$  and the frequency  $\omega_q$ :

$$N_q(t) = [S_p \rho]^{-1} S_p \{ \rho S^+(t) b_q^+ + b_q S(t) \}. \quad (2.2)$$

Here  $b_q^+$  and  $b_q$  are the phonon creation and annihilation operators,  $\rho$  is the density matrix, and  $S$  is the time-development operator:

$$S(t) = \exp(-iHt/\hbar), \quad (2.3)$$

where  $H$  is the total Hamiltonian of a system which consists of interacting electrons and phonons, and is located in an external electric field. We shall neglect the interaction between electrons and phonons due to the lattice anharmonicity, as we are concerned with the stronger (piezoelectric) interaction.

We shall carry out the initial averaging using the density matrix

$$\rho = \exp\left(-\frac{H_0 - \mu \hat{N}}{T}\right), \quad (2.4)$$

where  $H_0$  is the Hamiltonian of noninteracting electrons and phonons in the absence of the field,  $\hat{N}$  is the total electron number operator, and  $T$  is the thermostat temperature (in energy units).

As was pointed out in the Introduction, we shall be particularly interested in the quantity  $N_q$  at such  $q$  that

$$\hbar q \ll p, \quad \hbar \omega_q \ll \varepsilon_p. \quad (2.5)$$

If the quasi-classical conditions (2.5) and (2.1) are fulfilled, the diagram analysis of (2.2) becomes much simpler, as we shall see now. The graph representation of the Laplace transform  $N_q(s)$  of  $N_q(t)$

$$N_q(s) = \int_0^\infty dt e^{-st} N_q(t) \quad (2.6)$$

in the Konstantinov-Perel' technique is displayed in Fig. 1. Time goes from the left to the right—from 0 to  $t$  at the terminal points. The upper part of the contour is directed along the time (points of interaction from  $S(t)$  fall on here), and the lower part against the time (points from  $S^+(t)$ ). In the quasi-classical case, i.e., when (2.5) is satisfied, it is convenient to join the graphs which differ in the position of interaction points on either upper or lower halves of the contour. Let us consider the simplest process leading to phonon absorption (amplification), namely "conversion" of a phonon into an elec-

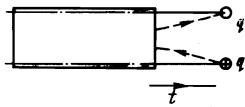


FIG. 1

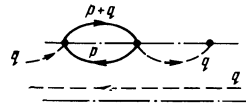


FIG. 2



FIG. 3

tron "pair" and back (Fig. 2). This diagram corresponds to the following analytic expression:

$$-ic_q \sum_p \frac{(1-f_{p+q})f_p}{s-i(\omega_q-\epsilon_{p+q}+\epsilon_p)} [-ic_q(n_q+1)]. \quad (2.7)$$

Here  $c_q$  is the electron-phonon interaction constant, and  $n_q$  and  $f_p$  are the equilibrium distribution functions of phonons and electrons;  $\hbar = 1$ .

There exist altogether four diagrams of this kind. They can be obtained by transferring in turn points 1 and 2 from the upper to the lower half of the contour. In so doing:

a) a transfer of point 2 (right-hand point) alters the correctness of the phonon line ( $n_q$  instead of  $n_q + 1$ ) and the sign (+i instead of -i);

b) a transfer of point 1 (left-hand point) alters the correctness of the electron lines ( $f_p \rightarrow f_{p+q}$  and vice versa) and the sign. Adding up these four diagrams and using the quasi-classical conditions (2.5) as well as the fact that  $f_p \ll 1$  (nondegenerate electrons) we have

$$\beta_q = ic_q \sum_p \frac{q \partial f_p / \partial p}{s-i\omega_p+iq v} (-ic_q). \quad (2.8)$$

We represent the sum of the four "quantum" diagrams, which yields (2.8), in the form of one "classical" diagram (see Fig. 3). Expression (2.8) corresponds to the thick line in the "classical" diagram—to an "electron arrow" carrying a frequency  $\omega_q$  and a momentum  $q$ . This is none other than an electron-concentration wave excited by a phonon. As we pass to the classical case, the contour becomes redundant: there remains only one type of ordering, namely the time ordering.

The collecting of the four quantum diagrams into one is the main point in deriving the classical technique. Now the quantum diagram chains contained in the block in Fig. 1 can also be represented as chains of classical objects—the electron arrows  $\beta_q$  and  $\beta_q^*$ —connected in series with phonon lines which do not carry the intensity  $n_q$  (Fig. 4). We note, however, that, as the earliest-in-time interaction point is transferred downwards, both the electron and the phonon lines change their correctness simultaneously (see Fig. 5). Therefore, two terms of the same order in the quasi-classical parameters will appear at this place:  $\beta_q n_q$  and the term

$$\alpha_q = c_q^2 \sum_p \frac{f_p}{s-i\omega_q+iq v}. \quad (2.9)$$

Thus, summation of the chains reduces to summation of the geometric progression, with the first term being either  $(\alpha_q + \alpha_q^*)$  or  $(\beta_q + \beta_q^*)n$ . This gives us the following expression for  $N_q(s)$ :

$$N_q(s) = \frac{n_q + (\alpha_q + \alpha_q^*)/s}{s - (\beta_q + \beta_q^*)} \quad (2.10)$$

or in the time representation:

$$N_q(t) = \gamma_q N_q + \mathfrak{A}_q, \quad (2.11)$$

where the coefficient of absorption (amplification) is

$$\gamma_q = 2\text{Re } \beta_q, \quad (2.12)$$

and the "source" is

$$\mathfrak{A}_q = 2\text{Re } \alpha_q. \quad (2.13)$$

In summing the chains we have neglected the diagrams with overlapping electron arrows (Fig. 6). In the case of overlapping, the free section  $1/s$  (see Fig. 4) is replaced by a non-free one (see Fig. 6) which is of order  $1/\omega_q$  (or  $1/q \cdot v$ ). Since in a geometric progression we must have  $s \geq \gamma$ , the neglect of overlapping arrows is justified for small damping (amplification), when

$$\gamma \ll \omega, \quad (2.14)$$

which thus furnishes a criterion for existence of the linear phonon kinetic equation (2.11). This criterion will be assumed satisfied.

The expressions obtained for the absorption coefficient and the source are applicable to the "collisionless" regime  $q l \equiv q v \tau_p \gg 1$ ,  $\omega \tau_p \gg 1$  in an equilibrium state. Let us now take into account the interaction of electrons with the thermostat (shortwave phonons and impurities) and the effect of the electric field. Since the criteria (2.1) and (2.5) are assumed for the electron system, the introduction of the field and the collisions reduces to, first, incorporation of the field term and of the collision integral in the collisionless propagators:

$$(s-i\omega_q+iqv)^{-1} \rightarrow (s-i\omega_q+iqv+I_p)^{-1}, \quad (2.15)$$

$$I_p = eE \partial / \partial p + I_p^{\text{th}},$$

and second, replacement of the equilibrium electron distribution function  $f_p$  by a non-equilibrium function  $F_p$  which obeys the equation

$$I_p F_p = 0. \quad (2.16)$$

Taking this into account, we shall henceforth depict our basic graphic object—the classical electron arrow—as in Fig. 7. The "tail" behind the left-hand interaction point will be correlated to the stationary electron distribution function  $F_p$  (the replacement of  $f_p$  by  $F_p$  is produced by "stretching out" the line corresponding to  $f_p$  in a graph of the type of Fig. 2 to the left beyond its left-hand connection point, and by "saturating" it there with points of interaction with the field and with the shortwave phonons).

We correlate the points in the diagram of Fig. 7 with  $\pm ic_q$  (the input point with +i and the output point with -i), the right-hand point with the summation over  $p$ , and the



FIG. 4



FIG. 5

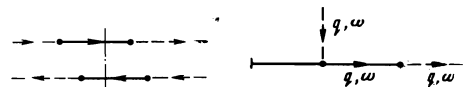


FIG. 6



FIG. 7

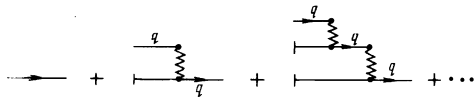


FIG. 8

left-hand point with  $q\partial/\partial p$  ( $q$  is the momentum entering the point). The line segment between the points corresponds to the propagator  $B_p^{-1}(q, \omega_q)$  where  $B_p(q, \omega_q)$  is the "response operator"

$$B_p(q, \omega) = -i\omega + iqv + I_p, \quad (2.17)$$

All the operators act to their left, i.e. on quantities which are preceding in time. Thus, the analytic expression for the diagram displayed in Fig. 7 is of the form

$$\beta_q = c_q^2 \sum_p B_p^{-1}(q, \omega_q) q \frac{\partial F_p}{\partial p}. \quad (2.18)$$

This diagram can be regarded as describing the process of excitation by a phonon of an electron density wave with its subsequent conversion into a phonon. For  $q \lesssim \chi$  ( $\chi$  is reciprocal of the Debye-Hückel radius) one also has to take into account the Coulomb interaction between electron density waves. This interaction is depicted graphically in Fig. 8. The double point of the Coulomb interaction corresponds to  $i4\pi e^2/q^2$ , and the other rules of correspondence remain the same as for the diagram of Fig. 7. The wave momentum and energy (frequency) are conserved in the course of interaction. Summation of the progression displayed in Fig. 8 will reduce to replacing the propagator  $B_p^{-1}(q; \omega_q)$  by  $\mathcal{B}_p^{-1}(q, \omega_q)$ , where the operator  $\mathcal{B}_p(q, \omega)$  is defined as follows ( $x_p$  being an arbitrary function of the quasi-momentum  $p$ ):

$$\mathcal{B}_p(q, \omega) x_p = B_p(q, \omega) x_p - i \frac{4\pi e^2}{q^2} q \frac{\partial F_p}{\partial p} \sum_p x_p. \quad (2.19)$$

This is the electron-system response operator with allowance made for the self-consistent field.

The linear absorption (amplification) coefficient of longwave phonons is given by a sum of the analytic expressions for the diagram of Fig. 7 and for its analog with the oppositely directed arrows (which yields the complex conjugate expression). The propagators between points correspond in this sum to  $\mathcal{B}_p^{-1}$  (or  $\mathcal{B}_p^{*-1}$  if the arrow opposes the direction of time). Thus, we have

$$\gamma_q = 2c_q^2 \operatorname{Re} \left\{ \sum_p \mathcal{B}_p^{-1}(q, \omega_q) q \frac{\partial F_p}{\partial p} \right\}, \quad (2.20)$$

or, introducing the longitudinal dielectric constant  $\epsilon_{q\omega}$ ,

$$\gamma_q = 2 \operatorname{Re} \left\{ \frac{c_q^2}{\epsilon_{q\omega}} \sum_p B_p^{-1}(q, \omega_q) q \frac{\partial F_p}{\partial p} \right\}, \quad (2.21a)$$

$$\gamma_q = - \frac{q^2}{4\pi e^2} \frac{c_q^2}{|\epsilon_{q\omega_q}|^2} \operatorname{Im} \epsilon_{q\omega_q}. \quad (2.21b)$$

Here

$$\epsilon_{q\omega} = 1 - i \frac{4\pi e^2}{q^2} \sum_p B_p^{-1}(q, \omega) q \frac{\partial F_p}{\partial p}. \quad (2.22)$$

The inclusion of the collisions and the field will also change the source  $\alpha_q$  in the equation for phonons (2.11). The diagram analysis shows that the change in the source can be incorporated by replacing (2.9) by (cf. also<sup>[8]</sup>):

$$\alpha_q = \frac{2c_q^2}{|\epsilon_{q\omega_q}|^2} \operatorname{Re} \left\{ \sum_p B_p^{-1}(q, \omega_q) F_p \right\}. \quad (2.23)$$

Having developed the graphical method using a simple example of linear amplification we shall now proceed to a nonlinear theory. Under the conditions of amplifica-

tion after a certain time<sup>2)</sup> the intensity of the longwave noises increases so much that they begin to affect the properties of the electron system. This, in turn, affects the amplification and the source in Eq. (2.11). In terms of the Konstantinov-Perel' diagram technique it means that one must fill the electron blocks with non-equilibrium longwave phonons—phonon lines carrying non-equilibrium intensities  $N_q$ .

As has been mentioned, the pairwise combination of graphs which differ in the position of either the input or the output point of the phonon line may give rise to a term like  $N_q q \partial/\partial p$ . Such a term appears if the transfer alters the correctness of the phonon line, i.e., at the points where the phonon line goes off to the right (or enters from the right). The source  $\alpha_q$  in the linear equation (2.11), which we discussed already, provides an example of such a term. The expression in braces in (2.23) is the correlator of the electron density fluctuations<sup>[8]</sup>. The higher-order terms in phonon nonlinearity will bring about more complex electron objects with many tails, i.e., higher-order electron correlation functions. However, if

$$N_q \hbar q / p \gg 1, \quad (2.24)$$

all these "spontaneous" terms can be neglected and one can construct a nonlinear diagram technique using simple objects—the above-introduced electron arrows and phonon lines.

Condition (2.24) implies a strongly non-equilibrium state when the phonon number considerably exceeds its equilibrium value. At equilibrium the rejected terms would exactly compensate the remaining nonlinear terms, and this would guarantee the required absence of nonlinear corrections to the fluctuation-dissipation theorem<sup>[9]</sup>. Far from equilibrium, on the other hand, only the maximal power of the intensity  $N_q$  should be retained at each power of the interaction constant, i.e., both the linear source and the nonlinear corrections to it should be rejected. This corresponds to neglect of generation of new phonons in a sufficiently amplified noise.

Let us briefly describe the principles of constructing a simple diagram technique under the conditions (2.24), (2.5), and (2.1). First, we take into account the influence of an increased noise on the stationary electron distribution function. In the first approximation in  $N_q$  this addition is given by two diagrams (Fig. 9). The phonon line corresponds in this diagram to  $N_q'$ . One of the interaction points is encircled. This means the renormalization of the electron-phonon interaction constant  $c_q \rightarrow c_q/\epsilon_{q\omega_q}$  (incoming phonon line),  $c_q \rightarrow c_q/\epsilon_{q\omega_q}$  (outgoing phonon line). The renormalization is a consequence of the Coulomb interaction between the electron waves (in addition to that incorporated in  $\mathcal{B}_p^{-1}$ ) (Fig. 10). Note that only the "inner" points on the electron arrows are renormalized (encircled); renormalization of the outer points (the nearest one to the "tail" and



FIG. 9

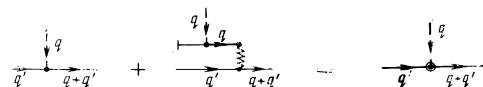


FIG. 10

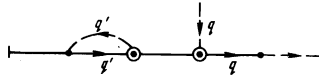


FIG. 11

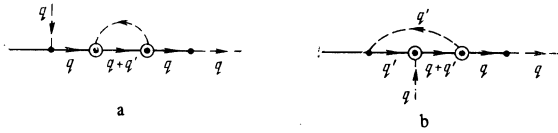


FIG. 12

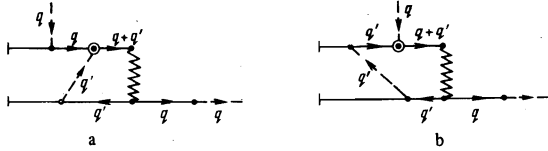


FIG. 13

the extreme right-hand point of an electron arrow) is done automatically by including the self-consistent field in  $\mathcal{B}_p(q, \omega)$  (in other words the processes leading to the renormalization are taken into account in the chain in Fig. 8; for this reason the linear theory involves  $c_q$  and not  $c_q/\epsilon_{\mathbf{q}\omega_{\mathbf{q}}}$ ).

The analytic expression for the sum of diagrams in Fig. 9 is of the form

$$\varphi_p = I_p^{-1} \sum_{\mathbf{q}} N_{\mathbf{q}} \frac{c_{\mathbf{q}}^2}{|\epsilon_{\mathbf{q}\omega_{\mathbf{q}}}|^2} [B_p^{-1}(\mathbf{q}, \omega_{\mathbf{q}}) + B_p^{*-1}(\mathbf{q}, \omega_{\mathbf{q}})] \mathbf{q} \frac{\partial F_p}{\partial \mathbf{p}} \quad (2.25)$$

(the extreme right-hand electron segment with zero momentum is, according to (2.17), set in correspondence with  $I_p^{-1}$ ). If  $q_l \gg 1$  and  $\omega\tau_p \gg 1$ , the electron-phonon interaction proceeds like a collision

$$B_p^{-1} + B_p^{*-1} = 2\pi\delta(\omega - qv). \quad (2.26)$$

The contribution to the amplification due to the change in the distribution function can be obtained by replacing the tail in the linear diagram of one of the diagrams in Fig. 9 (see Fig. 11). This is only one of the diagrams describing the effect of the phonon  $\mathbf{q}'$  on the amplification of  $\mathbf{q}$ . Two other diagrams are displayed in Fig. 12. To those we must also add the diagrams with two electron waves which cannot be reduced to a renormalization of  $c_q$  (see Fig. 13). Diagrams a in Fig. 12 and 13 represent corrections to the electron propagator due to the presence of enhanced noise. Diagram b gives corrections to the interaction (to the vertex part). Let us formulate the correspondence rules once again.

Phonon lines (except for those incoming or outgoing from the extreme right-hand point of an electron arrow) correspond to the non-equilibrium intensity  $N_{\mathbf{q}}$ . All  $\mathbf{q}$ , except for those pointing outwards, are summed over. The entering points of phonon lines correspond to  $ic_{\mathbf{q}}/\epsilon_{\mathbf{q}\omega_{\mathbf{q}}}$  (or to  $ic_{\mathbf{q}}$  if a point is not encircled), and the double point of "input" of the Coulomb interaction corresponds to  $i4\pi e^2/q^2$ . Every point on an electron arrow, except for the extreme right-hand one, corresponds to an operator  $\mathbf{q}\partial/\partial\mathbf{p}$ , where  $\mathbf{p}$  is the momentum that enters (or leaves) the electron arrow at this point; the extreme right-hand point corresponds to the summation over  $\mathbf{p}$ . Each segment of an electron arrow pointing to the right corresponds to an operator  $B_p^{-1}(\Sigma\mathbf{q}, \Sigma\omega_{\mathbf{q}})$ , where  $\Sigma\mathbf{q}$  and  $\Sigma\omega_{\mathbf{q}}$  are the algebraic sums of momenta and frequencies of the phonons which "constitute" the electron segment

involved. Output points and the leftward arrows correspond to the complex conjugate quantities. The tail of an electron arrow corresponds to  $F_p$ .

Thus, the kinetics of longwave strongly non-equilibrium [according to the criterion (2.24)] phonons is described by a simple graphic technique. Its elements are phonon lines of two kinds: those that carry intensities and those that do not. The time ordering of the interaction points, which is essential for this technique, is always present in the kinetics in one form or another. We also note that the two kinds of phonon lines (carrying and not carrying intensity) are inevitable in the classical diagram technique (cf. [1]). They stem from the expressions for  $N_{\mathbf{q}} + 1$  (emission) and  $N_{\mathbf{q}}$  (absorption) which are inherent in the quantum statistics.

The structure of the extended vertices of the phonon-phonon interaction depends on the particulars of this interaction. In our case of the interaction via the electron subsystem these vertices assume the simplest form for  $q \gg \chi$ , when one can neglect the Coulomb interaction between the electron-density waves. In this case the extended phonon-phonon interaction vertex is represented by a single electron arrow consisting of the electron-system propagators with electron-phonon interaction points in between.

In order to illustrate the correspondence rules, we write down the analytic expressions for diagrams a and b in Fig. 12:

$$\sum_{\mathbf{q}'} \frac{c_{\mathbf{q}}^2 c_{\mathbf{q}'}^2 N_{\mathbf{q}'}}{|\epsilon_{\mathbf{q}\omega_{\mathbf{q}}}|^2} \sum_{\mathbf{p}} \mathcal{B}_p^{-1}(\mathbf{q}, \omega_{\mathbf{q}}) \mathbf{q}' \frac{\partial}{\partial \mathbf{p}} \mathcal{B}_p^{-1}(\mathbf{q} + \mathbf{q}', \omega_{\mathbf{q}} + \omega_{\mathbf{q}'}) \cdot \mathbf{q}' \frac{\partial}{\partial \mathbf{p}} \mathcal{B}_p^{-1}(\mathbf{q}, \omega_{\mathbf{q}}) \mathbf{q} \frac{\partial F_p}{\partial \mathbf{p}}, \quad (2.27)$$

$$\sum_{\mathbf{q}'} \frac{c_{\mathbf{q}}^2 c_{\mathbf{q}'}^2 N_{\mathbf{q}'}}{\epsilon_{\mathbf{q}\omega_{\mathbf{q}}} \epsilon_{\mathbf{q}'\omega_{\mathbf{q}'}}} \sum_{\mathbf{p}} \mathcal{B}_p^{-1}(\mathbf{q}, \omega_{\mathbf{q}}) \mathbf{q}' \frac{\partial}{\partial \mathbf{p}} \mathcal{B}_p^{-1}(\mathbf{q} + \mathbf{q}', \omega_{\mathbf{q}} + \omega_{\mathbf{q}'}) \cdot \mathbf{q} \frac{\partial}{\partial \mathbf{p}} \mathcal{B}_p^{-1}(\mathbf{q}', \omega_{\mathbf{q}'}) \mathbf{q}' \frac{\partial F_p}{\partial \mathbf{p}} \quad (2.28)$$

and diagram b in Fig. 13:

$$\sum_{\mathbf{q}'} \frac{c_{\mathbf{q}}^2 c_{\mathbf{q}'}^2 N_{\mathbf{q}'}}{\epsilon_{\mathbf{q}\omega_{\mathbf{q}}} \epsilon_{\mathbf{q}'\omega_{\mathbf{q}'}}} \frac{4\pi e^2}{(\mathbf{q} + \mathbf{q}')^2} \sum_{\mathbf{p}} \mathcal{B}_p^{-1}(\mathbf{q}, \omega_{\mathbf{q}}) (\mathbf{q} + \mathbf{q}') \frac{\partial}{\partial \mathbf{p}} \cdot \mathcal{B}_p^{-1}(\mathbf{q}', \omega_{\mathbf{q}'}) \mathbf{q}' \frac{\partial F_p}{\partial \mathbf{p}} \sum_{\mathbf{p}'} \mathcal{B}_{p'}^{-1}(\mathbf{q} + \mathbf{q}', \omega_{\mathbf{q}} + \omega_{\mathbf{q}'}) \mathbf{q} \frac{\partial}{\partial \mathbf{p}'} \cdot \mathcal{B}_{p'}^{-1}(\mathbf{q}', \omega_{\mathbf{q}'}) \mathbf{q}' \frac{\partial F_{p'}}{\partial \mathbf{p}'}. \quad (2.29)$$

By reversing the direction of  $\mathbf{q}'$  in the diagrams in the diagrams in Figs. 11–13 we obtain five more expressions which completely account for the first correction to the amplification factor.<sup>3)</sup> The next (in intensity) correction can be obtained by including one more phonon line in the diagrams of the first correction. The ratio of each two successive corrections is of the order of magnitude of

$$\frac{\gamma}{\omega} \frac{1}{n_0 V_0} \sum_{\mathbf{q}} N_{\mathbf{q}} \frac{\hbar q}{p} \sim \frac{\kappa^3}{n_0} \frac{\gamma}{\omega} \frac{N_{\mathbf{q}}}{n_{\mathbf{q}}}$$

(where  $V_0$  is the volume,  $n_0$  is the electron concentration,  $\chi$  is the reciprocal Debye radius, and  $n_{\mathbf{q}}$  is the equilibrium number of phonons). We can confine ourselves to the first corrections in intensity if the latter parameter is sufficiently small. In this case the equation for  $N_{\mathbf{q}}$  can be written in the form

$$N_{\mathbf{q}} = (\gamma_{\mathbf{q}} + \sum_{\mathbf{q}'} W_{\mathbf{q}\mathbf{q}'} N_{\mathbf{q}'}) N_{\mathbf{q}}. \quad (2.30)$$

We shall not display here the analytic expression for

$W_{\mathbf{q}\mathbf{q}'}$  which is rather unwieldy, since the graphs for the first correction, which determines  $W_{\mathbf{q}\mathbf{q}'}$ , have been already listed.

### 3. HYDRODYNAMIC APPROXIMATION

Evaluation of the amplification factor requires knowledge of the operator  $\mathcal{B}_{\mathbf{p}}^{-1}(\mathbf{q}, \omega)$ , i.e. the solution of the corresponding response equation. Let us consider the case of long waves  $ql \ll 1$ ,  $\omega\tau_p \ll 1$ , when the inversion of  $\mathcal{B}_{\mathbf{p}}(\mathbf{q}, \omega)$  is trivial. Indeed, in this "hydrodynamic" limit we have a simple algorithm<sup>[10]</sup>

$$\mathcal{B}_{\mathbf{p}}^{-1}(\mathbf{q}, \omega)y_{\mathbf{p}} = \left[ F_{\mathbf{p}} - iqI_{\mathbf{p}}^{-1}(v-V)F_{\mathbf{p}} + i\frac{4\pi e^2 n_0}{q^2} qI_{\mathbf{p}}^{-1} \frac{\partial F_{\mathbf{p}}}{\partial \mathbf{p}} \right] - iq \sum_{\mathbf{p}'} v' I_{\mathbf{p}'}^{-1} y_{\mathbf{p}'}/n_0 \quad (3.1)$$

$$\times \frac{1}{4\pi\sigma + q^2 D - i(\omega - \mathbf{q}\mathbf{V})} + I_{\mathbf{p}}^{-1} y_{\mathbf{p}}.$$

The function  $y_{\mathbf{p}}$  has the property  $\sum_{\mathbf{p}} y_{\mathbf{p}} = 0$  (electron number conservation). In (3.1) we have introduced the following notation:

$$D_{ik} = \sum_{\mathbf{p}} v_i I_{\mathbf{p}}^{-1}(v_k - V_k) F_{\mathbf{p}}/n_0,$$

for the non-equilibrium diffusion tensor,

$$\sigma_{ik} = -e^2 \sum_{\mathbf{p}} v_i I_{\mathbf{p}}^{-1} \partial F_{\mathbf{p}} / \partial p_k$$

for the differential conductivity tensor, and  $\mathbf{V} = \sum_{\mathbf{p}} \mathbf{v} F_{\mathbf{p}} / n_0$  for the drift velocity ( $n_0 = \sum_{\mathbf{p}} F_{\mathbf{p}}$ ). The dielectric constant  $\epsilon_{\mathbf{q}\omega}$  is given in this approximation by

$$\epsilon_{\mathbf{q}\omega} = \frac{4\pi\sigma + q^2 D - i(\omega - \mathbf{q}\mathbf{V})}{q^2 D - i(\omega - \mathbf{q}\mathbf{V})}. \quad (3.2)$$

(In (3.1), (3.2), and below  $\sigma$  and  $D$  are the projections of the corresponding tensors on the direction of  $\mathbf{q}$ .)

In the hydrodynamic limit all the terms that are nonlinear in  $I^{-1}$  should be neglected. Hence, when the algorithm (3.1) is applied repeatedly, only the first term in brackets in (3.1) proves to be significant. Thus, the electron distribution function  $F_{\mathbf{q}}$  is carried all the way through the expression

$$\mathcal{B}_{\mathbf{p}}^{-1}(\mathbf{q}, \omega) q' \frac{\partial F_{\mathbf{p}}}{\partial \mathbf{p}} = F_{\mathbf{p}} \frac{i(\mathbf{q}\mu\mathbf{q}')}{4\pi\sigma + q^2 D - i(\omega - \mathbf{q}\mathbf{V})}. \quad (3.3)$$

Since in the end we always have to sum over  $\mathbf{p}$ , the final expressions contain the concentration  $n_0$  instead of  $F_{\mathbf{p}}$ . For convenience, we have introduced one more quantity  $\mu_{ik} = \sigma_{ik}/e^2 n_0$ , i.e., the differential mobility per unit force.

Now we can readily write down the hydrodynamic expressions directly from the diagrams, modifying the correspondence rules in the following way:

1) replacing the propagator  $\mathcal{B}_{\mathbf{p}}^{-1}(\mathbf{q}, \omega)$  by  $i\mathcal{B}_{\mathbf{q}\omega}^{-1}$  where

$$\mathcal{B}_{\mathbf{q}\omega} = 4\pi\sigma + Dq^2 - i(\omega - \mathbf{q}\mathbf{V}) = 4\pi\sigma + B_{\mathbf{q}\omega}; \quad (3.4)$$

2) replacing the derivative  $q' \partial / \partial \mathbf{p}$  by  $(\mathbf{q}\mu\mathbf{q}')$ , where  $\mathbf{q}$  is the propagator momentum after (i.e., to the right of) the point at which the momentum  $\mathbf{q}'$  enters (leaves) the line;<sup>4)</sup>

3) the "tail" corresponds to  $n_0$  rather than  $F_{\mathbf{p}}$ ; summation over  $\mathbf{p}$  at the right-hand point of the electron arrow is omitted;

4)  $\epsilon_{\mathbf{q}\omega}$  is given by (3.2).

As an illustration, in the linear theory we get (see Fig. 7 and Eq. (2.20)):

$$\gamma_{\mathbf{q}} = 2 \operatorname{Re} \left\{ \frac{n_0 c_{\mathbf{q}}^2 i(\mathbf{q}\mu\mathbf{q})}{\mathcal{B}_{\mathbf{q}\omega}} \right\}. \quad (3.5)$$

For diagram a in Fig. 12 we have

$$i^3 \sum_{\mathbf{q}'} \frac{n_0 c_{\mathbf{q}}^2 c_{\mathbf{q}'}^2 N_{\mathbf{q}'}(\mathbf{q}\mu\mathbf{q}')(\mathbf{q} + \mathbf{q}', \mu\mathbf{q}')(\mathbf{q}\mu\mathbf{q})}{|\epsilon_{\mathbf{q}'\omega_{\mathbf{q}'}}|^2 \mathcal{B}_{\mathbf{q}\omega}^2 \mathcal{B}_{\mathbf{q}+\mathbf{q}', \omega_{\mathbf{q}+\mathbf{q}'}}} \quad (3.6)$$

In the hydrodynamic limit the diagrams describing the effect of the change in the stationary distribution function (Fig. 11) become insignificant since they contain the zero-momentum electron segment which corresponds to  $I_{\mathbf{p}}^{-1}$ . The sum of the remaining eight diagrams gives the correction to the amplification factor in the hydrodynamic approximation:<sup>5)</sup>

$$\Delta\gamma_{\mathbf{q}} = \sum_{\mathbf{q}'} W_{\mathbf{q}\mathbf{q}'} N_{\mathbf{q}'} = 2 \operatorname{Re} \left\{ \sum_{\mathbf{q}'} \frac{i^3 n_0 c_{\mathbf{q}}^2 c_{\mathbf{q}'}^2 N_{\mathbf{q}'}}{|\epsilon_{\mathbf{q}'\omega_{\mathbf{q}'}}|^2 \mathcal{B}_{\mathbf{q}\omega}^2 \mathcal{B}_{\mathbf{q}+\mathbf{q}', \omega_{\mathbf{q}+\mathbf{q}'}}} \right. \\ \times [B_{\mathbf{q}'\omega_{\mathbf{q}'}}(\mathbf{q}\mu\mathbf{q})(\mathbf{q} + \mathbf{q}', \mu\mathbf{q}') + B_{\mathbf{q}\omega}(\mathbf{q}'\mu\mathbf{q}')(\mathbf{q} + \mathbf{q}', \mu\mathbf{q})] \\ \left. \times \left[ B_{\mathbf{q}'\omega_{\mathbf{q}'}}(\mathbf{q}\mu\mathbf{q}') + \frac{4\pi e^2 n_0}{(\mathbf{q} + \mathbf{q}')^2} (\mathbf{q}'\mu\mathbf{q}')(\mathbf{q}\mu, \mathbf{q} + \mathbf{q}') \right] + \left( \begin{array}{c} \mathbf{q}' \rightarrow -\mathbf{q}' \\ \omega_{\mathbf{q}'} \rightarrow -\omega_{\mathbf{q}'} \end{array} \right) \right\}.$$

If we took the imaginary part instead of the real, we would obtain the nonlinear correction to the sound velocity.

### 4. REMARKS ON DEVELOPED PHONON TURBULENCE

If the noise intensity is sufficiently enhanced ( $\chi^3 \gamma N_{\mathbf{q}} / n_0 \omega_{\mathbf{q}} \geq 1$ ), we cannot apply the perturbation theory to the evaluation of the nonlinear amplification factor and must sum over all the diagrams. The whole set of diagrams can be naturally broken down into three classes: change in the distribution function, change in the propagator, and renormalization of the interaction. Let us first consider the propagator. All the diagrams yielding corrections to the propagator are subdivided into irreducible and reducible ones (the latter are those which can be cut without intersecting the phonon line). We denote the sum of all irreducible diagrams, displayed in Fig. 14, by  $\mathfrak{M}_{\mathbf{q}}(\mathbf{q}, \omega_{\mathbf{q}})$ . The propagator itself, which we denote by  $\mathfrak{D}_{\mathbf{q}}^{-1}(\mathbf{q}, \omega)$ , is the sum shown in Fig. 15. Summing this series we find

$$\mathfrak{D}_{\mathbf{p}}(\mathbf{q}, \omega) = \mathcal{B}_{\mathbf{p}}(\mathbf{q}, \omega) + \mathfrak{M}_{\mathbf{p}}(\mathbf{q}, \omega). \quad (4.1)$$

This is the new operator of ("instantaneous") response in our system.<sup>6)</sup>

Acting in a similar way, we obtain an equation for the ("quasi-stationary") electron distribution function:

$$(I_{\mathbf{p}} + \mathfrak{M}_{\mathbf{p}}) F_{\mathbf{p}} = 0. \quad (4.2)$$

The operator  $\mathfrak{M}_{\mathbf{p}}$  which appears here is  $\mathfrak{M}_{\mathbf{p}}(\mathbf{q}, \omega)$  at  $\mathbf{q} = 0$  and  $\omega = 0$ . It remains to introduce the new vertex part instead of the old simple point (see Fig. 16). The arising expression is convenient to denote by

$$ic_{\mathbf{q}} \mathbf{q} \Gamma_{\mathbf{p}}(\mathbf{q}, \omega) \partial / \partial \mathbf{p} \quad (4.3)$$

( $\mathbf{q}$  and  $\partial / \partial \mathbf{p}$  contain all the diagrams of the sum;  $\Gamma$  is a tensor.



FIG. 14

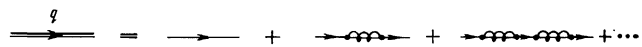


FIG. 15

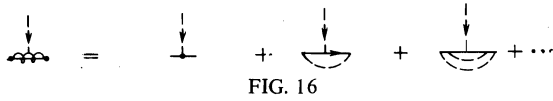


FIG. 16

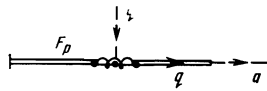


FIG. 17

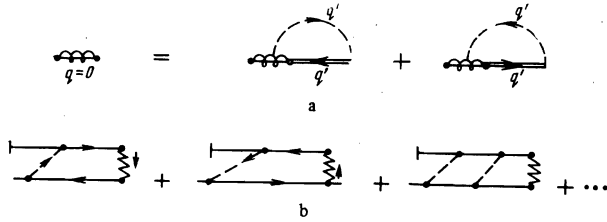


FIG. 18

Let us now express the noise amplification factor in terms of the above-introduced symbols  $\mathcal{L}_p$ ,  $\Gamma_p$ , and  $F_p$ . According to Fig. 17, it is equal to

$$\gamma_q^n = 2c_q^2 \operatorname{Re} \left\{ \sum_p \mathcal{L}_p^{-1}(q, \omega_q) q \Gamma_p(q, \omega_q) \partial F_p / \partial p \right\}. \quad (4.4)$$

The quantities  $\mathcal{L}$ ,  $\Gamma$ , and  $\mathfrak{M}$  are connected by certain relations, which can be readily obtained with the help of the diagrams representing these quantities. For example, at  $q \gg \chi$  we obtain the following expression for  $\mathfrak{M}_p$  (cf. Fig. 18, a):

$$\mathfrak{M}_p = - \left\{ \sum_q c_q^2 N_q q \frac{\partial}{\partial p} \mathcal{L}_p^{-1}(q, \omega_q) q \Gamma_p(q, \omega_q) \frac{\partial}{\partial p} + \text{c.c.} \right\}. \quad (4.5)$$

The similar expressions for  $\mathfrak{M}_p(q, \omega)$  and  $\Gamma_p(q, \omega)$  involve more complex formations, which in turn can be related to even more complex ones. Such a chain may be useful in principle for approximating  $\mathfrak{M}$ ,  $\mathcal{L}$ , and  $\Gamma$  in an evaluation of the nonlinear amplification factor. Such a calculation itself seems to be very involved and we shall not be concerned here with this problem.

An attempt to go beyond the framework of the perturbation theory in the hydrodynamic limit was made by Wonnerberger<sup>[5, 17]</sup>. He took into account the changes in the propagator and ignored the vertex part renormalization (corrections the distribution function are insignificant in the hydrodynamic limit). We observe, however, that in a perturbation theory calculation (see Secs. 2 and 3) the contribution due to the vertex renormalization (see Figs. 12, b and 13, b) is of the same order of magnitude as that of corrections to the propagator (Figs. 12, a and 13, a)—cf., say, (2.28) and (2.27). When considering the higher-order diagrams in the noise intensity there is also no reason to prefer processes that lead to a variation in the propagator to those associated with the vertex part renormalization. For this reason, Wonnerberger's work cannot be regarded as consistent.

The summand in (4.4) is (to within a factor of  $i$ ) the response function relating the variation  $\delta F_p(q, \omega)$  of the electron distribution to a weak (and sufficiently fast!) potential perturbation  $\delta u(\mathbf{z}, t) = \delta u_{q\omega} \exp(-i\omega t + i\mathbf{q} \cdot \mathbf{r})$  acting on the electron system:

$$\begin{aligned} \delta F_p(q, \omega) &= R_p(q, \omega) \delta u_{q\omega}, \\ R_p(q, \omega) &= i \mathcal{L}_p^{-1}(q, \omega) q \Gamma_p(q, \omega) \partial F_p / \partial p. \end{aligned} \quad (4.6)$$

The sum over  $p$  of  $R_p(q, \omega)$  is the response  $R_{q\omega}$ :

$$\delta n_{q\omega} = R_{q\omega} \delta u_{q\omega}. \quad (4.7)$$

Thus, the noise amplification factor is proportional to the imaginary part of the response function:

$$\gamma_q^n = 2c_q^2 \operatorname{Im} R_{q\omega}. \quad (4.8)$$

Instead of the response  $R_{q\omega}$  one can introduce the dielectric constant

$$\tilde{\epsilon}_{q\omega}^{-1} = 1 + 4\pi e^2 q^{-2} R_{q\omega}. \quad (4.9)$$

Then  $\gamma_q^n$  and  $\tilde{\epsilon}_{q\omega}$  turn out to be connected by the formula (2.21b), which thus acquires a more universal character.

In the case under consideration, the amplification factor  $\gamma_q^n$  is hard to calculate but, in principle, easy to measure. To do so, it suffices, say, to measure the amplification of a weak acoustic signal induced in the system. As seen from (4.8), the result will coincide exactly to the  $\gamma_q^n$  we are interested in. The reason for this coincidence is that the noise amplification is fairly uniform over the spectrum and the properties of the medium vary under the influence of a very large number of noise components, the influence of a particular single component being small compared to that of the totality of other components (the self-action is small compared to the interaction). Under these conditions, the contribution to  $\gamma_q^n$  due to phonons with the same  $q$  is small compared to that due to all other phonons, giving rise to a peculiar "linearization" of the problem.

An often used method of registration of the acoustic noise is to measure the acousto-electric current. The latter is defined as the difference between the values of current in the presence and in the absence of the noise. In our notation (see (4.2))

$$j_a^{ac} = e \sum_p v_a (F_p - \mathcal{F}_p) = -e \sum_p v_a I_p^{-1} \mathfrak{M}_p F_p. \quad (4.10)$$

Let first  $q \gg \chi$ . Then, substituting (4.5) in (4.10) and comparing with (4.4), we find that in the hydrodynamic approximation

$$j_a^{ac} = - \frac{1}{en_0} \sigma_{ab} \sum_q q_b \gamma_q^n N_q. \quad (4.11)$$

Now let us show that this formula holds for an arbitrary relation between  $q$  and  $\chi$ . At  $q \lesssim \chi$  the expression for  $\mathfrak{M}_p$  becomes more complicated as the right-hand side of the equation depicted in Fig. 18, a gets in addition the Coulomb terms shown in Fig. 18, b. However, in the hydrodynamic limit, due to factorization, these terms mutually cancel one another having oppositely directed momenta at the Coulomb vertex.

Eq. (4.11) means that Weinreich's relation holds true in the case of a developed acoustic turbulence as well.

## 5. LIMITS OF APPLICABILITY OF THE KINETIC EQUATION FOR PHONONS, AND ANALYSIS OF THE INTERACTION IN A NARROW BEAM

The nonlinear interaction picture in a noise growing in a wide spectrum region is not too complicated in principle, in so far as it is described by a closed kinetic equation of the form

$$\dot{N}_q - \gamma_q^n N_q = 0,$$

where  $\gamma_q^n$ , although being an intricate function, depends only on the intensities  $N_{q'}$ . However, in the course of amplification, due to various reasons (say, due to the

presence of sharp maxima in the amplification curve, or under certain experimental conditions, the amplified-phonon distribution over  $q$  may become drastically non-uniform. In this case, the "self-action" (i.e. the nonlinear interaction between phonons with very close values of wave-vector  $q$ , which is unimportant in a wide beam) becomes tangible. The fact that the "self-action" occurs differently from the "interaction" has been pointed out already in<sup>[4]</sup>. It was shown there that the coefficient, at the intensity in the nonlinear correction to the signal amplification factor is by no means equal to the diagonal part  $W_{qq}$  of the noise amplification. With the help of our diagram technique we can analyze this dissimilarity, namely find the processes which, playing no role in a wide beam, become significant on its narrowing.

An example of such a process is given in Fig. 19. In the derivation of Eq. (2.30) we neglected such processes, since their contribution is  $\gamma/\omega$  times smaller than that of the included ones. Indeed, compared to, say, the diagram in Fig. 12, a, the diagram in Fig. 19 contains, for one thing, two more interaction constants and one more propagator (which altogether gives  $\gamma$ ), and for another, an additional cut between the electron arrows. This cut brings about the factor  $[s + i(\omega_{q+q'} - \omega_q - \omega_{q'})]^{-1}$  which in a wide beam is of order  $1/\omega$ , whereas in a narrow one, when  $q' \rightarrow q$ , is equal to  $[s + i(\omega_{2q} - 2\omega_q)]^{-1}$ . If  $\omega_{2q} = 2\omega_q$ , this factor is large and compensates the smallness in the numerator (since  $s \sim \gamma$ ). By this means the contribution due to such a process becomes significant. Other diagrams of this type, whose contribution grows on narrowing of the beam, are displayed in Fig. 20. The sum of these four "growing" diagrams at  $q' = q$  is given (in the hydrodynamic limit) by the expression

$$\frac{8n_0^2 c_q^4 c_{2q}^2 N_q q^2 \mu \cdot B_{q\omega_q} (2B_{q\omega_q} - B_{2q, 2\omega_q})}{B_{2q, 2\omega_q}^2 \beta_{q\omega_q}^2 |\beta_{q\omega_q}|^2 i \Xi_q}, \quad (5.1)$$

where  $\Xi_q$  is a resonance denominator; with allowance made for the renormalization it is equal to

$$\Xi_q = \omega_{2q} - 2\omega_q + \frac{4n_0 c_{2q}^2 q^2 \mu}{B_{2q, 2\omega_q}} - \frac{2n_0 c_q^2 q^2 \mu}{B_{q\omega_q}}. \quad (5.2)$$

Diagrams of this type differ from those considered before in that each electron arrow here contains three rather than four electron-phonon interaction points. If we collect all the diagrams of this type (there are 18 of them altogether, but only four do grow) made up of three-phonon "vertices"—the electron waves, we get a collision term of the Peierls type. In a wide beam all

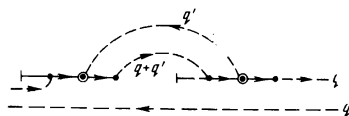


FIG. 19

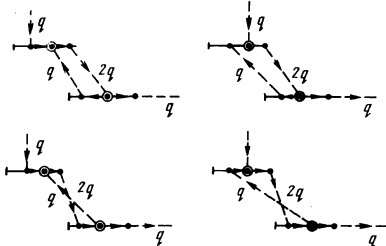


FIG. 20

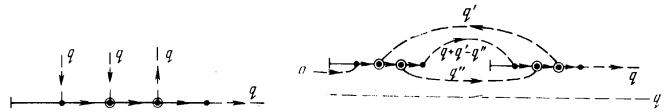


FIG. 21

these diagrams are small compared to the four-phonon (non-Peierls) ones. The fact of smallness of the Peierls terms for the nonlinear interaction in a growing noise in piezo-semiconductors was first established in<sup>[4]</sup>. Now we see that the Peierls terms are small only in a wide noise beam, whereas on narrowing of the beam some of the Peierls terms (the indicated four diagrams) increase and by the order of magnitude become equal to the non-Peierls one.

Let us note that if, for some reason, the four-phonon non-Peierls interaction is absent in the system, then the beam narrowing will give rise to an extremely drastic (of the order of  $\omega/\gamma$ ) change in the nonlinear interaction (which under these circumstances would be purely Peierls). In the instance of plasma this situation was recently discussed in an interesting work by Fisher and Hirshfield<sup>[11]</sup>.

The enhanced Peierls diagrams correspond to an interaction via the second harmonic in the nonlinear theory of the sound signal amplification.<sup>[6]</sup> If the dispersion of the sound velocity is large, so that  $\omega_{2q} \neq 2\omega_q$ , then the Peierls terms do not grow as the beam gets narrow (and for the signal case there is no interaction via the second harmonic). However, even in this simpler case Eq. (2.30) becomes unsuitable on narrowing of the beam. A comparison between the non-Peierls terms in a signal and in a noise (for  $q = q'$ ) shows that they agree to within a factor of 2. There is no accident in the occurrence of this factor: it reflects a profound difference between the statistical properties of a noise and a signal. The dissimilar behaviour of a coherent and incoherent radiation is well-known in the nonlinear optics<sup>[12]8</sup>: the  $n$ -th order nonlinear effects for an incoherent (Gaussian) source are  $n!$  times higher than the same effects for a coherent radiation.<sup>9</sup> Our situation is completely analogous in this sense. It is particularly apparent from diagrams for the signal amplification factor. The interaction procedure for solving the system of equations for a sound signal interacting with an electron density (see<sup>[6]</sup>) can be represented in a diagram form with the help of the above-introduced symbols. The nonlinear diagrams for the signal amplification will differ from those for the noise only in that their acoustic (phonon) lines are unclosed. (An example of such a graph is displayed in Fig. 21). Closing these lines, we get the former noise diagrams. The number of ways to close an  $n$ -th order diagram equals exactly  $n!$

Let us find out now which of the processes (besides the Peierls ones) disregarded in the derivation of (2.30) become important as the beam gets narrow. An example of an increasing non-Peierls diagram is given in Fig. 22. The four-phonon electron arrows in it are connected to each other by more than one phonon line. Let us compare this diagram with that (Fig. 23) incorporated in Eq. (2.30), which describes a successive interaction of a given phonon with two other ones (through waves of the electron density). The new diagram in Fig. 22 describing the simultaneous phonon interaction, and the old one in Fig. 23 differ in the section between the electron waves (which expresses the conservation of energy,



FIG. 23

or frequency, of phonons). For the old diagram this section equals  $1/s$ , for the new  $(s - i\Delta\omega)^{-1}$ , where  $\Delta\omega = \omega_{\mathbf{q}} + \omega_{\mathbf{q}'} - \omega_{\mathbf{q}''} - \omega_{\mathbf{q}+\mathbf{q}'-\mathbf{q}''}$ . If the spectrum is wide (the spread of  $\omega_{\mathbf{q}}$  is of the order of  $\omega_{\mathbf{q}}$  itself), then the ratio of the contributions of these diagrams is by the order of magnitude equal to  $s/\omega \approx \gamma/\omega \ll 1$  ( $s \sim \gamma$  is the reciprocal of the evolution time of the phonon system) and hence only the successive interaction is essential. Thus, the validity criterion for Eq. (2.30) is

$$\Delta\omega \gg \gamma. \quad (5.3)$$

For  $\Delta\omega \sim \gamma$  the contribution of the new diagram is of the same order as that of the old one, and for the self-action  $\mathbf{q} = \mathbf{q}' = \mathbf{q}''$  these contributions are exactly the same.

The phonon energy in our system is determined to within  $\gamma$ . Thus, the criterion  $\Delta\omega \gg \gamma$  implies that the interaction prevails over the self-action. The self-action, which increases as the beam gets narrower, can produce more radical changes in the phonon system than the nonlinear interaction accounted for in (2.30). For example, the processes shown in Fig. 22 (and more complicated ones of the same type) are responsible for the change of the statistical properties of the phonon system in a transition from noise to signal. The latter question, which is little connected to the specific character of a piezo-semiconductor (i.e. to the concrete type of the wave interaction), will be considered by us separately. Here we note only that inclusion of the simultaneous self-action at  $\mathbf{q}' = \mathbf{q}$  eliminates the factorial factors from the expansion of the nonlinear amplification factor in powers of the intensity  $N_{\mathbf{q}}$  (for the first nonlinear correction, this is the above-mentioned factor of 2). Besides another disparity between the signal and the noise amplification factors, which is rather subtle, disappears at  $\mathbf{q}' = \mathbf{q}$ : namely, the resonance denominator (see (5.2)) for the growing Peierls terms contains the sum of the linear amplification factors  $\gamma 2_{\mathbf{q}} + 2\gamma_{\mathbf{q}}$ , whereas the corresponding expression for signal<sup>[6]</sup> involves the difference  $\gamma 2_{\mathbf{q}} - 2\gamma_{\mathbf{q}}$ .<sup>10)</sup>

The authors are pleased to express their gratitude to V. L. Gurevich and B. D. Laikhtman for numerous discussions and valuable critical remarks. The authors are grateful to A. G. Aronov, O. V. Konstantinov, and V. L. Perel' for an interesting discussion.

<sup>1)</sup>It is interesting to note that the Peierls terms correspond in the limit to the interaction via the second harmonic in a coherent wave, described in [6].

<sup>2)</sup>It is more convenient for us to consider the spatially-uniform case.

The transition to a more realistic situation of the spatially-growing noise is trivial.

- <sup>3)</sup>The direction of  $\mathbf{q}'$  need not be reversed since this would merely produce the complex conjugate to the expression already derived. One should just take twice the real part of the latter.
- <sup>4)</sup>The diagrams should be read from future to past, i.e. from the right to the left; therefore, the order of the symbols in the formulae is opposite to that of elements in the diagrams. If the tensor  $\mu_{jk}$  is symmetrical (which is not true in general), then the order of  $\mathbf{q}$  and  $\mathbf{q}'$  is immaterial.
- <sup>5)</sup>The results coincide with that calculated in [4] by another method, if  $\sigma_{jk}$  in [4] is understood as the differential conductivity and  $\chi^2$  is defined as equal to  $4\pi\sigma/D$ .
- <sup>6)</sup>The phonon system evolves slowly compared to the electron one. The operator  $\mathbf{e}_p$  varies with the rate of this evolution and describes the response to a rapid perturbation of frequency  $\omega \gg \gamma$ .
- <sup>7)</sup>Wonneberger starts with an equation for the electron density in an acoustic field and, subsequently, averages it. The diagram technique obtained is similar to ours.
- <sup>8)</sup>We are grateful to V. I. Perel' who drew our attention to these works.
- <sup>9)</sup>There is no "coherent-incoherent" mysticism in this factorial; just the possible large intensities in a Gaussian source contribute more to the nonlinear effects than to its mean intensity.
- <sup>10)</sup>This disparity reflects the difference in the interaction procedures applied: for the case of noise, the sum of the coefficients results, roughly speaking, from the integration over time of the product  $u_{2\mathbf{q}}^* u_{\mathbf{q}}$ , whereas for signal the difference appears in the solution of the equation of motion for  $u_{2\mathbf{q}}$ , which contains  $u_{\mathbf{q}}$  in the right-hand side.

<sup>1)</sup>H. W. Wyld, Ann. Phys. (N. Y.) 14, 143 (1961).

<sup>2)</sup>V. N. Tsyтович, Nelineinye efekty v plazme (Nonlinear Effects in Plasma), Nauka, 1967.

<sup>3)</sup>A. A. Galeev and V. I. Karpman, Zh. Eksp. Teor. Fiz. 44, 592 (1963) [Sov. Phys.-JETP 17, 403, 1963].

<sup>4)</sup>V. L. Gurevich, V. D. Kagan, and B. D. Laikhtman, Zh. Eksp. Teor. Fiz. 54, 188 (1968) [Sov. Phys.-JETP 27, 102 (1968)].

<sup>5)</sup>W. Wonneberger, Z. Naturforsch. A26, 1625 (1971).

<sup>6)</sup>V. L. Gurevich and B. D. Laikhtman, Zh. Eksp. Teor. Fiz. 49, 960 (1965) [Sov. Phys.-JETP 22, 668 (1966)].

<sup>7)</sup>O. V. Konstantinov and V. I. Perel', Zh. Eksp. Teor. Fiz. 39, 197 (1960) [Sov. Phys.-JETP 12, 142 (1961)].

<sup>8)</sup>S. V. Gantsevich, V. L. Gurevich, and R. Katilyus, Zh. Eksp. Teor. Fiz. 59, 533 (1970) [Sov. Phys.-JETP 32, 291 (1971)].

<sup>9)</sup>S. M. Rytov, Vvedenie v statisticheskuyu radiofiziku (Introduction to the Statistical Radiophysics) Nauka, 1966, p. 294.

<sup>10)</sup>S. V. Gantsevich, V. L. Gurevich, and R. Katilyus, Zh. Eksp. Teor. Fiz. 57, 503 (1969) [Sov. Phys.-JETP 30, 276 (1970)]; S. V. Gantsevich, V. L. Gurevich, and R. Katilyus, Phys. Cond. Matter, 1974.

<sup>11)</sup>R. K. Fisher and J. L. Hirshfield, Phys. Fluids 16, 567 (1973).

<sup>12)</sup>P. Lambropoulos, C. Kikuchi, and R. K. Osborn, Phys. Rev. 144, 1081 (1966); V. A. Kovarskiĭ, Zh. Eksp. Teor. Fiz. 57, 1217 (1969) [Sov. Phys.-JETP 30, 663 (1970)].

Translated by S. Luryi

192